

University of Richmond

UR Scholarship Repository

Honors Theses

Student Research

4-29-2022

Synthesis and Study of Unsymmetrical Bidentate Bis(phosphino)pyrrole Ligands and Their Transition Metal Complexes

Julia F. Vidlak
University of Richmond

Follow this and additional works at: <https://scholarship.richmond.edu/honors-theses>



Part of the [Organic Chemistry Commons](#), and the [Polymer Chemistry Commons](#)

Recommended Citation

Vidlak, Julia F., "Synthesis and Study of Unsymmetrical Bidentate Bis(phosphino)pyrrole Ligands and Their Transition Metal Complexes" (2022). *Honors Theses*. 1650.
<https://scholarship.richmond.edu/honors-theses/1650>

This Thesis is brought to you for free and open access by the Student Research at UR Scholarship Repository. It has been accepted for inclusion in Honors Theses by an authorized administrator of UR Scholarship Repository. For more information, please contact scholarshiprepository@richmond.edu.

Synthesis and Study of Unsymmetrical Bidentate Bis(phosphino)pyrrole Ligands and Their
Transition Metal Complexes

by

Julia F. Vidlak

Honors Thesis

Submitted to:

Chemistry Department
University of Richmond
Richmond, VA

April 29, 2022

Advisor: Dr. Miles Johnson

Abstract

Our laboratory has reported the synthesis and characterization of a broad library of unsymmetrical bidentate bis(phosphino)pyrrole (BPP) ancillary ligands for use in nickel-catalyzed cross-coupling reactions. The electronic and steric properties of nickel complexes bearing these ligands are examined, and our data support the hypothesis that these ligands produce nickel complexes with electron-deficient metal centers. The syntheses of (BPP)Ni(*o*-tolyl)Cl precatalysts for utilization in nickel-catalyzed Buchwald-Hartwig Amination are described, and preliminary reactivity studies reveal that (BPP)Ni(*o*-tolyl)Cl precatalysts are effective in promoting C–N cross-coupling reactions. Finally, we report steric measurements and electronic properties obtained from computed (BPP)NiCl₂ and (BPP)Ni(CO)₂ complexes, respectively. Additional reactivity studies to correlate changes in ancillary ligand characteristics with success in nickel catalysis are underway.

Introduction

Transition metal catalyzed cross-coupling reactions have led to major breakthroughs in synthetic chemistry.¹ With the aid of a metal catalyst, cross-coupling reactions form C–C, C–O, and C–N bonds with a variety of starting materials at high yields and purities. Buchwald-Hartwig Amination (BHA) is arguably one of the most successful metal-catalyzed cross-coupling reactions. This palladium mediated reaction couples aryl halides with amines and was developed simultaneously in the Buchwald and Hartwig laboratories in 1995.^{2,3} Since its development, BHA has become the 11th most frequently used reaction in medicinal chemistry and has broad applications to the fields of process chemistry and materials science.^{4,5}

Metal-catalyzed transformations have traditionally utilized metals such as palladium, rhodium, ruthenium, and iridium as catalysts. However, the cost, toxicity, and low relative abundance⁶ of these precious metals have pushed the synthetic community to develop equally effective catalysts with earth-abundant metals.⁷ One candidate that has become increasingly popular for use in BHA is nickel. In comparison to palladium, which is traditionally utilized in BHA, nickel is cheaper and has a significantly lower environmental impact. While increased research focused on nickel catalysis has improved the metal's performance in C–N cross-coupling, harnessing the reactivity of nickel can be challenging. In comparison to palladium, nickel is known to occupy a larger range of oxidation states (0 to +4), therefore increasing the complexity of possible mechanistic pathways.⁸ While the formation of Ni(I) and Ni(III) species through single electron transfer (SET) pathways could potentially increase the scope of products formed in cross-coupling, these species can also inhibit two electron transfer mechanisms such as those involved in BHA.^{9, 10}

The key to the development of nickel-catalyzed amination reactions is in the rational design of ligands designed specifically for nickel. Despite the presented challenges associated with the reactivity of nickel, researchers have generally studied nickel catalysis with ligands that have been successful for palladium cross-coupling with varying amounts of success. While ligands such as BINAP¹¹ and dppf¹² can mediate nickel-catalyzed BHA, the classic monodentate dialkylbiaryl phosphines developed in the Buchwald laboratory for palladium-catalyzed BHA do not work for nickel.¹³ From recent studies of nickel-catalyzed BHA, notably the work of Stradiotto and coworkers, it is evident that the rational design of ancillary ligands for nickel is essential for improving nickel catalysts.¹⁴⁻¹⁸ Specifically, designing electron-deficient ligands that can promote rate-limiting reductive elimination in addition to studies that interrogate how the individual steric and electronic properties of ancillary ligands promote or hinder catalytic performance will allow

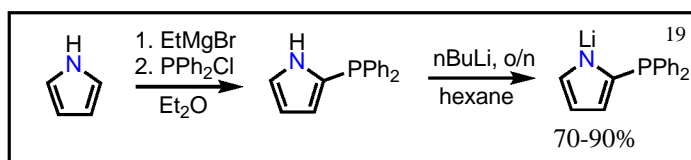
for the improvement of nickel catalysts and a greater understanding of the elementary steps involved in Ni(0)/Ni(II) and Ni(I)/Ni(III) mechanistic pathways.

Given the results of these previous studies and a lack of sustainable synthetic routes for the synthesis of bisphosphines, our laboratory sought to design a diverse library of electron-deficient ligands that could be synthesized with accessible starting materials for use in nickel-catalyzed BHA. Herein, we report the modular synthesis of unsymmetrical bidentate bis(phosphino)pyrrole ligands (BPP) and their nickel complexes, a comparative study of the steric and electronic properties of nickel BPP complexes, and evidence that precatalysts coordinated with BPP ligands can promote C–N cross-coupling reactions. In addition, Density Functional Theory (DFT) studies of modeled nickel BPP complexes are discussed.

Results and Discussion

Ligand Library Synthesis

Following the synthetic procedure outlined by Tonks and coworkers,¹⁹ 2-diphenyl(phosphino)pyrrolide was prepared as shown (Figure 1). The steps leading to the synthesis of 2-diphenyl(phosphino)pyrrole produce a mixture of species, including products resulting from the addition of diphenylphosphine to the 1 and 3 position of pyrrole. These species are easily separated by column chromatography with the desired product being obtained by crystallization. Treating 2-diphenyl(phosphino)pyrrole with 1.6 equiv. of *n*BuLi in hexanes followed by filtration affords lithium 2-diphenyl(phosphino)pyrrolide at approximately 70-90% yield.



Advantages

- Modular
- Inexpensive starting materials
- No Pd cross-coupling

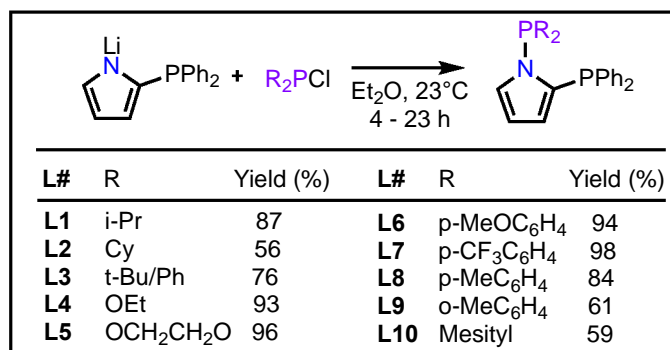


Figure 1. Ligand library synthesis.

Stirring lithium pyrrolide with a chlorophosphine in diethyl ether followed by crystallization generates the desired bidentate bis(phosphino)pyrrole ligand. From this synthetic procedure, ten ligands with varying steric and electronic properties were accessed in moderate to excellent yield (Figure 1). This ligand library includes sterically hindered ligands **L10** (R = Mesityl) and **L9** (R = *o*-tolyl), in addition to electron-deficient ligands including **L7** (R = *p*-CF₃) and the phosphoramidites **L4** and **L5**.

Comparative Studies

Following the synthesis of the ligand library, a comparative study of BPP ligands with their phenylene analogs was performed to investigate the steric and electronic profiles of BPP ligands relative to ligands that are widely used in cross-coupling reactions. Aryl phosphine derivatives such as dialkylbiaryl phosphines, DalPhos, and ferrocene derivatives are frequently utilized in C–N cross-coupling reactions.¹³ Therefore, the phenylene analog of **L1**, **L11**, was prepared from the literature precedent²⁰ for utilization in the following comparative studies (Figure 2). We hypothesized that nickel complexes derived from **L1** would be electron-deficient relative to their phenylene congeners due to incorporation of electron withdrawing nitrogen into the bidentate phosphine backbone.

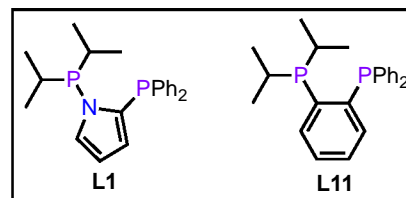


Figure 2. **L1** and **L11**.

Synthesis of NiCl₂ and Ni(CO)₂ Complexes

NiCl₂ and Ni(CO)₂ complexes derived from **L1** and **L11** were synthesized for utilization in the comparative study (Figure 3). X-ray quality crystals of the NiCl₂ complexes were obtained by DCM/pentane layering (Figure 4).

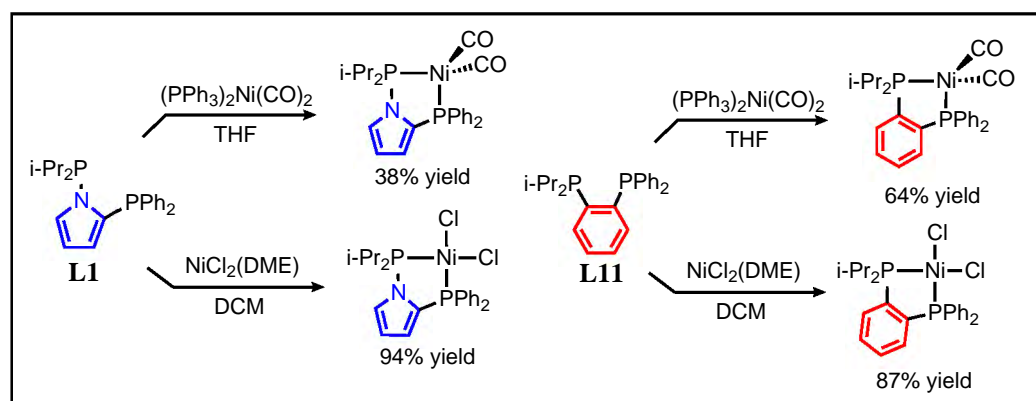


Figure 3. Synthesis of NiCl₂ and Ni(CO)₂ complexes with **L1** and **L11**.

Steric Parameters

Comparison of the crystal structures obtained from the two nickel dichloride complexes reveals similar steric profiles for both complexes (Table 1). A 1.131° difference in bite angle exists between the pyrrole and phenylene linkers, and the complexes have a 0.7% difference in percent buried volume. Percent buried volume measures the amount of volume a ligand occupies within a sphere of a given radius.²¹ Analysis of the steric maps produced by the SambVca program shows similar regions of relative steric bulk for the two complexes (Figure 4).

Further inspection of the NiCl₂ crystal structures reveals information related to the trans influence of the two complexes, specifically through analysis of the Ni–Cl bond trans to Pi-Pr₂ (Table 1). In the solid state, this bond is 0.03 Å shorter for (**L1**)NiCl₂ in comparison to the analogous bond in the (**L11**)NiCl₂ complex. Since Pi-Pr₂ is directly bound to the pyrrolyl nitrogen, the observed difference reveals that the pyrrolyl nitrogen is likely weakening the trans influence of the Pi-Pr₂ donor. As a result, BPP ligands could serve as a tool for researchers interested in modifying the

trans influence of bidentate phosphine ligands while retaining a similar steric profile to phenylene-based phosphine ligands.

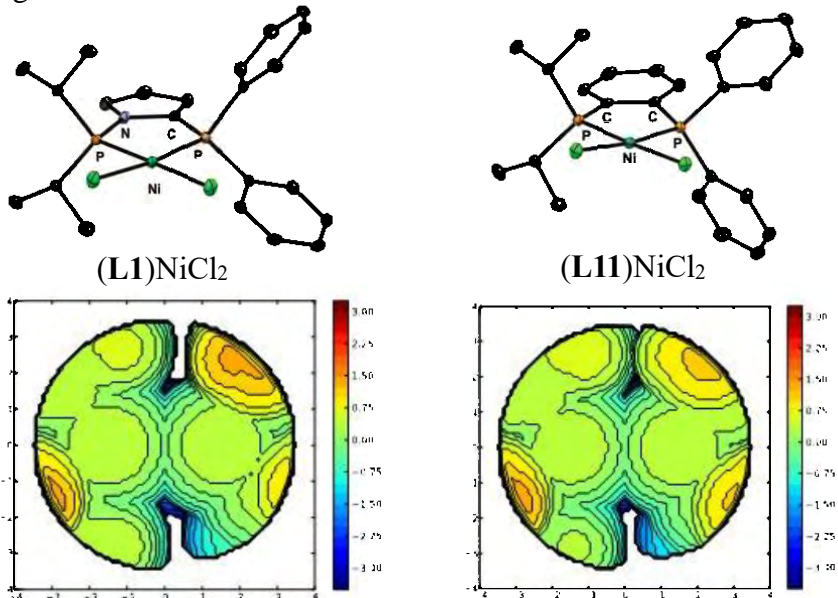


Figure 4. Crystal structures and steric maps of **(L1)NiCl₂** and **(L11)NiCl₂**. Ellipsoids are shown at 50% probability. Hydrogens and solvent molecules are excluded for clarity.

	(L1)NiCl₂	(L11)NiCl₂
Bite angle (X = Cl)	89.66(3)°	88.53(2)°
%V _{bur}	54.5%	55.2%
Ni–Pi–Pr ₂	2.1382(8) Å	2.1585(4) Å
Ni–PPh ₂	2.1418(7) Å	2.1348(4) Å
Ni–Cl trans to Pi–Pr ₂	2.1880(7) Å	2.2190(4) Å
Ni–Cl trans to PPh ₂	2.2024(8) Å	2.1949(4) Å

Table 1. Measured steric properties of **(L1)NiCl₂** and **(L11)NiCl₂**.

Electronic Properties

The electronic properties of the NiCl₂ complexes were obtained and compared, including HOMO-LUMO gap energy with UV-Vis spectroscopy and reduction potential with cyclic voltammetry. The CO stretching frequencies of the Ni(CO)₂ complexes were measured with IR spectroscopy. The results of these studies are summarized in Table 2.

	(L1)NiX₂	(L11)NiX₂
v _{max} (X = Cl)	456 nm	454 nm
E _{red} (vs. Fc ⁺⁰) (X = Cl)	–1.6 V	–1.7 V
v _{CO} (X = CO)	1996, 1934 cm ^{–1}	1986, 1924 cm ^{–1}

Table 2. Measured electronic properties of **(L1)NiCl₂**, **(L11)NiCl₂**, **(L1)Ni(CO)₂** and **(L11)Ni(CO)₂**.

(**L1**)NiCl₂ was found to be reduced at a potential 0.1 V more positive in comparison to the phenylene complex. In agreement with our hypothesis, this difference suggests that Ni(BPP) complexes are more electron-deficient than their phenylene analogs, as (**L1**)NiCl₂ was more easily reduced in comparison to (**L11**)NiCl₂. The CO stretching frequencies of the Ni(CO)₂ complexes further corroborate the electron deficiency of Ni(BPP) complexes relative to their phenylene congeners. $\Delta\nu_{\text{CO}}$ was found to be 10 cm⁻¹ higher for (**L1**)Ni(CO)₂ in comparison to (**L11**)Ni(CO)₂. This result indicates that there is less back-bonding between the nickel center and the CO ligands for (**L1**)Ni(CO)₂ resulting in a comparatively higher carbonyl stretching frequency. Lastly, the difference in ligand backbone does not significantly perturb the HOMO-LUMO gap, with $\Delta\nu_{\text{max}} = 2$ nm.

Summary of Comparative Studies

The comparative studies reveal that Ni(BPP) complexes retain similar steric profiles in comparison to their phenylene congeners with attenuated electron donation. As a result, cross-coupling reactions with a rate-limiting reductive elimination step, including nickel-catalyzed BHA, could benefit from the use of these electron-deficient ligands.¹⁴⁻¹⁸ These results prompted us to test the reactivity of **L1** in BHA.

Synthesis of **L1**Ni(*o*-tolyl)Cl Complex **C1** and Reactivity in Buchwald-Hartwig Amination

Following the general synthetic procedure outlined by Doyle and coworkers,²² **L1**Ni(*o*-tolyl)Cl complex **C1** was synthesized from the precursor complex (TMEDA)Ni(*o*-tolyl)Cl (Figure 5). Crystallization with DCM/pentane layering afforded the desired analytically pure complex and crystals for X-ray diffraction. **C1** was utilized to test the general reactivity of pyrrole ligands. The reaction coupling 4-chlorobenzonitrile with furfurylamine was selected for this purpose, as this C–N coupling reaction is heavily benchmarked in the literature.²³⁻²⁷ Performing this reaction in triplicate with 5 mol % catalyst loading of **C1** at 25 °C generated the coupled product at a 71 ± 2% yield (average of three runs). Increasing the temperature to 40 °C resulted in complete conversion to product. These results indicate that BPP ligands can perform a challenging cross-coupling reaction with comparable results to several established ligands with more elaborate synthetic protocols.²³⁻²⁷ The results of the above syntheses and studies of unsymmetrical bidentate bis(phosphino)pyrrole ligands were reported by our laboratory in 2020.²⁸

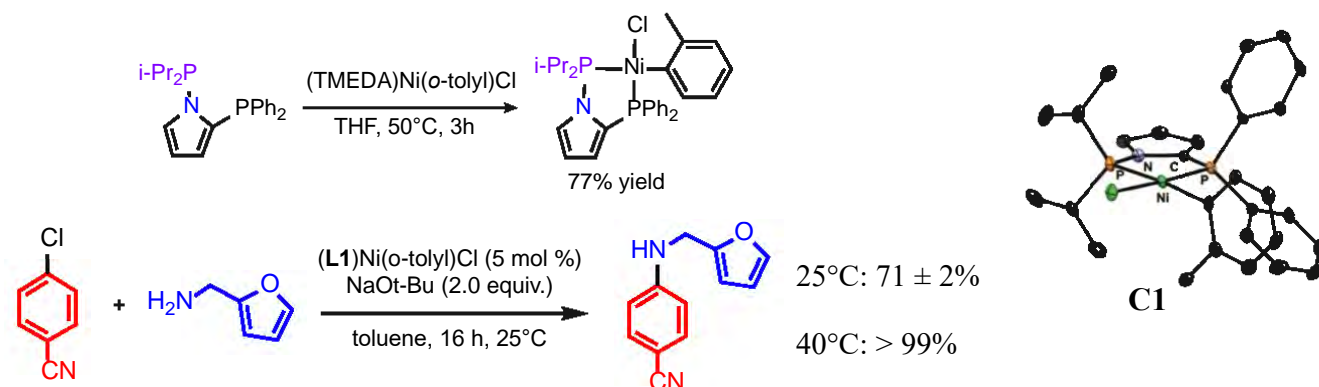


Figure 5. Synthesis of **C1** and reactivity in BHA. Crystal structure of **C1**. Ellipsoids are shown at 50% probability. Hydrogens and solvent molecules are excluded for clarity.

Synthesis of $L_nNi(o\text{-tolyl})Cl$ Complexes

Following the synthesis of **C1**, the synthetic procedures of several precatalysts derived from additional ligands in the ligand library have been established through small scale reactions monitored by NMR. The general procedure for these reactions involves treating a THF/ d_6 -benzene solution of 0.025 mmol ligand with 1 equiv. (TMEDA)Ni(*o*-tolyl)Cl in a J. Young tube and then observing the reaction progress by NMR. Figure 6 shows how a typical reaction is monitored by ^{31}P NMR using **L3** as a model. Preliminary yields and reaction conditions are presented in Table 3. Several complexes required temperatures up to 50 °C over extended periods of time to reach completion, while other complexes were successfully formed at room temperature including **C6** and **C7**.

Due to our initial observation that **C1** is air-stable, all work-up procedures were initially performed open to air. These first syntheses revealed that several (BPP)Ni(*o*-tolyl)Cl precatalysts, including **C7**, **C8**, and **C10**, are air sensitive while precatalysts derived from **C2**, **C3**, and **C6** are air-stable as evidenced by indications of decomposition or lack thereof in the NMR spectra. In addition to variability in air-sensitivity, several complexes exist as mixtures of isomers, as the chlorine and *o*-tolyl ligands can interchange positions. The isomers are observed as two sets of doublets in the ^{31}P NMR spectra (Figure 6, expanded region on right). Crystal structures were obtained for **C2**, **C3**, and **C6** (Figure 7).

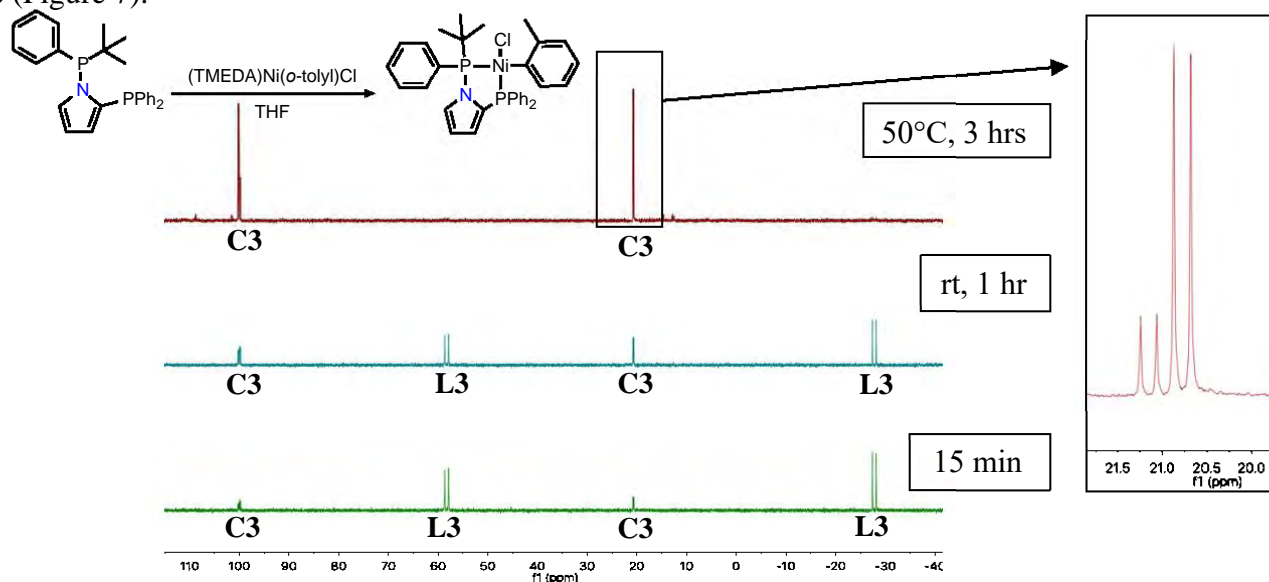


Figure 6. ^{31}P NMR of small scale (0.025 mmol) reaction of **L3** with (TMEDA)Ni(*o*-tolyl)Cl.

Complex (BPP Ligand)	Time	Temperature	Yield	Approx. Isomer Ratio	Air-stable?
C2 (Cy)	o/n	50 °C	93%	-	Y
C3 (<i>t</i> -Bu/Ph)	3 hrs	50 °C	81%	1:5	Y
C6 (<i>p</i> -MeO)	2 hrs	rt	78%	1:2	Y
C7 (<i>p</i> -CF ₃)	2 hrs	rt	TBD	-	N
C8 (<i>p</i> -Me)	1 hr	50 °C	TBD	1:2	N
C10 (Mes)	16 hrs	45 °C	49%	-	N

Table 3. Summary of preliminary syntheses of (BPP)Ni(*o*-tolyl)Cl precatalysts.

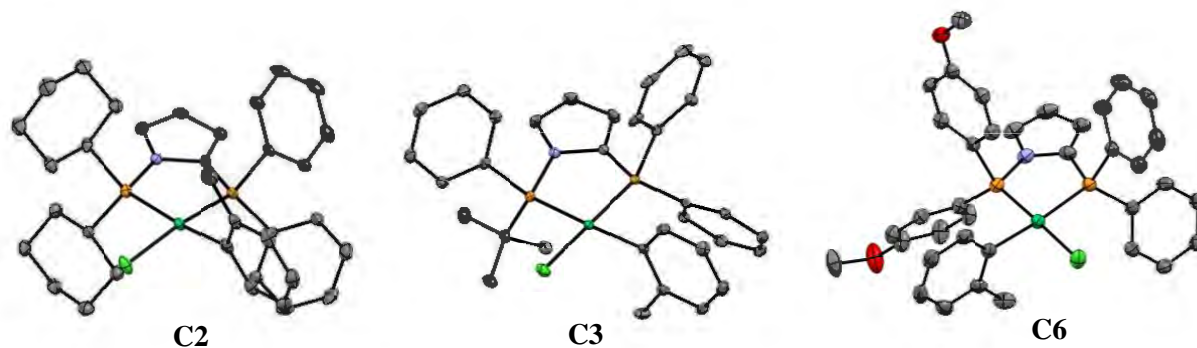


Figure 7. Crystal structures of air-stable precatalysts **C2**, **C3**, and **C6**. Ellipsoids are shown at 50% probability. Hydrogens and solvent molecules are excluded for clarity.

Computational Studies with $L\#NiCl_2$ and $L\#Ni(CO)_2$ Complexes

To determine how ligand properties impact catalytic performance, it was important to first have a means to quantitatively compare the relative steric and electronic properties of the BPP derivatives. In thinking about how phosphine ligands have been compared historically, Tolman's parameters are classically cited.²⁹ Tolman compared the properties of monodentate phosphine ligands through the synthesis of tricarbonyl nickel complexes coordinated with a large variety of monodentate phosphines. Tolman then plotted each complex with respect to its carbonyl stretching frequency (the electronic parameter) on the y-axis and its cone angle (the steric parameter) on the x-axis to generate Tolman's parameters.

Inspired by Tolman's parameters, we turned to Density Functional Theory (DFT) to create a similar comparison. Using Gaussian 16 and the B3LYP^{30,31}/ccpvtz^{32,33} level of theory, optimization and frequency calculations were performed with modeled nickel dichloride and nickel dicarbonyl complexes derived from **L1-L10** ($L\#NiCl_2$, $L\#Ni(CO)_2$). Using carbonyl stretching frequency as the electronic parameter and percent buried volume as the steric parameter, we were able to compare each ligand in our ligand library as shown (Figure 8). These data serve as an important reference to quantitatively correlate ligand properties with percent yield in catalysis for each cross-coupling reaction that we study.

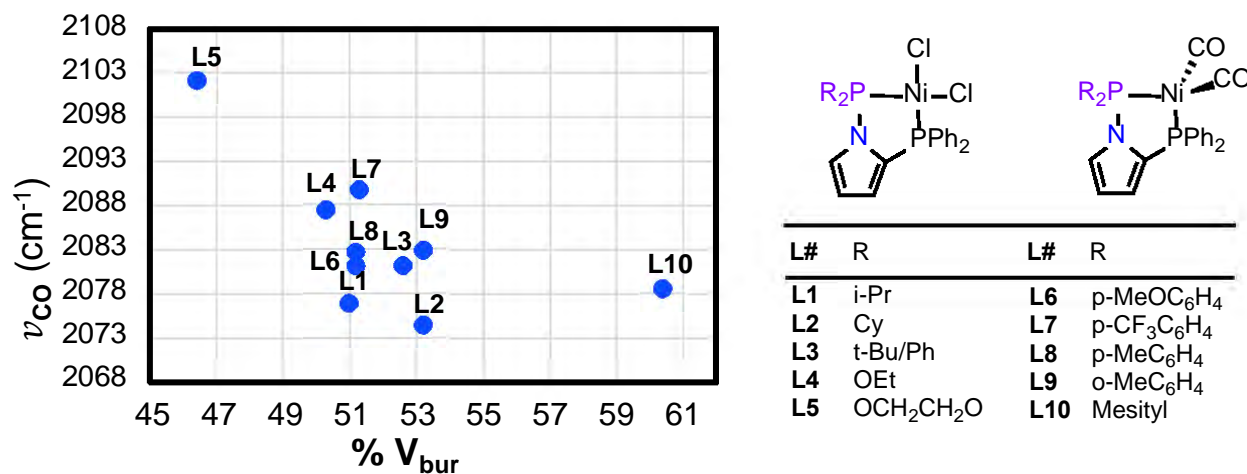
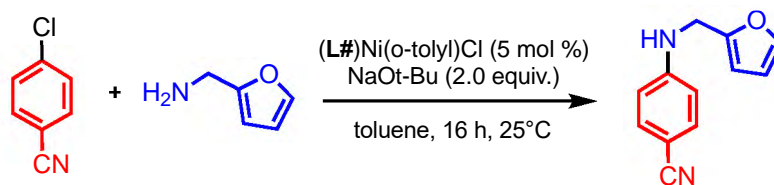


Figure 8. Results of computed steric and electronic measurements with carbonyl stretching frequency on the y-axis and percent buried volume on the x-axis.

Preliminary Reactivity Studies

In this ongoing study, the catalytic performance of precatalysts derived from BPP derivatives in BHA coupling of furfurylamine and 4-chlorobenzonitrile have been studied, with our results summarized in Table 4.



C# (BPP Ligand)	Yield ^a	%V _{bur} ^b	N
C1 ²⁸ (i-Pr)	71	51.0	3
C2 (Cy)	92	53.2	2
C3 (tBu/Ph)	91	52.6	2
C10 (Mes)	93	60.3	1

Table 4. Results of preliminary reactivity studies. ^a Determined by NMR. ^b From DFT. N = number of runs. Determined yield is the average value obtained from N runs.

From these initial studies, it appears that increasing the steric bulk of the ancillary phosphine generally increases catalytic performance. We observed a 21% increase in yield from **C1** to **C2** which was accompanied by a 2.2% increase in percent buried volume. No significant increase in catalytic performance was observed from **C2/C3** to **C10**. These results agree with the Stradiotto group's finding that electron-poor and bulky ligands aid to promote nickel-catalyzed aryl-N reductive elimination.¹⁵⁻¹⁸ In future studies, we hope to further analyze the impact of ancillary ligand electronic properties on catalytic yield with the *p*-substituted BPP nickel precatalysts.

Conclusions

We report the synthesis and study of a diverse library of ten bidentate bis(phosphino)pyrrole ligands. The use of affordable starting materials, the avoidance of C–P palladium cross coupling, and the modular synthetic route utilized for the generation of the ligand library are all advantages of this synthesis over the syntheses of several well established bisphosphines. Through a comparative study, we were able to gather sufficient evidence supporting the electron-deficient nature of BPP ligands relative to their phenylene analogs. This property could potentially aid in promoting rate-limiting reductive elimination in nickel-catalyzed BHA. These ligands can promote a challenging C–N cross-coupling reaction between furfurylamine and 4-chlorobenzonitrile, and our preliminary reactivity studies suggest that increasing steric bulk improves catalytic performance. Finally, through DFT studies, we have developed a model based on Tolman's parameters that compares the steric and electronic properties of BPP ligands through the calculation of percent buried volume and carbonyl stretching frequency of (BPP)NiCl₂ and (BPP)Ni(CO)₂ complexes, respectively. Future studies aim to examine the impact of electronic properties on catalysis through the utilization of the *p*-substituted BPP ligands, in addition to increasing the scope of substrates used in catalytic studies.

Experimental

General Considerations. All reactions were carried out in a nitrogen-filled MBraun LABstar Pro glovebox unless otherwise stated. All glassware was oven-dried overnight at greater than 110 °C and cooled under vacuum prior to use. Anhydrous hexane, pentane, and dichloroethane (DCE) were purchased from Aldrich and stored over 3 Å molecular sieves prior to use. All other solvents were collected from a Glass Contour Solvent Purification System, degassed, and stored over 3 Å molecular sieves in a glovebox. Dichloromethane-*d*₂ (CD₂Cl₂) was purchased from Cambridge Isotope Laboratories and stored over 3 Å molecular sieves. Lithium 2-(diphenylphosphino)pyrrolide¹⁹ and 1-(diphenylphosphino)-2-(diisopropylphosphino)benzene²⁰ were prepared according to literature procedures. Tetrabutylammonium hexafluorophosphate ([*n*-Bu₄N][PF₆]) for electrochemical studies was recrystallized three times from ethanol. Filtrations were performed using PTFE syringe filters with 0.45 μm pores. The chlorophosphines *i*-Pr₂PCl (Fisher or Sigma Aldrich), (*o*-tolyl)₂PCl (Strem), (EtO)₂PCl (Fisher), Cy₂PCl (Acros), Ph(*t*-Bu)PCl (Strem), (2,4,6-trimethylphenyl)₂PCl (Sigma-Aldrich), (*p*-CF₃C₆H₄)₂PCl (Alfa Aesar), (*p*-CH₃C₆H₄)₂PCl (Alfa Aesar), (C₂H₄O₂)₂PCl (Fisher), (MeOC₆H₄)₂PCl, *t*-Bu₂PCl (Alfa Aesar), and Ph₂PCl (Aldrich) were used as received from their respective vendors. The transition metal complexes (DME)NiCl₂, (TMEDA)Ni(*o*-tolyl)Cl, and (Ph₃P)₂Ni(CO)₂ were used as received from Strem Chemicals. For catalytic studies, furfurylamine (Fisher) was distilled from CaH₂ and stored over 3 Å molecular sieves, and 4-chlorobenzonitrile (Oakwood) and ferrocene (99%, Strem) were used as received.

Spectroscopy. ¹H, ¹³C{¹H}, ¹⁹F{¹H}, and ³¹P{¹H} spectra were collected on Bruker AV-300, AV-400, and AV-500 NMR spectrometers at ambient temperature. ¹H NMR chemical shifts (δ) are reported in parts per million (ppm) relative to the solvent (5.32 ppm for CDHCl₂). ¹³C NMR spectra were referenced relative to the solvent signal (53.84 ppm for CD₂Cl₂). ³¹P{¹H} and ¹⁹F{¹H} were referenced using the absolute reference function of the Mnova 9.0.1 NMR software package. Infrared spectra were recorded on a Nicolet iS10 FT-IR spectrometer. UV-vis data were acquired using a Cary 60 UV-vis spectrophotometer.

X-ray Crystallography. X-ray crystallographic data were collected on a Rigaku Oxford Diffraction Supernova diffractometer. Crystal samples were handled under immersion oil and quickly transferred to a cold nitrogen stream.

Electrochemistry. Electrochemical experiments were performed inside a glovebox in tetrahydrofuran (THF) with 0.1 M [*n*-Bu₄N][PF₆] and 1 mM analyte. A CH Instruments 660E potentiostat was used with a 3 mm glassy carbon working electrode and a platinum wire auxiliary electrode. The silver wire reference electrode was referenced to the ferrocene-ferrocenium couple.

Elemental Analysis. Elemental analyses were performed by Midwest Microlab, LLC.

For Ligand Library Synthesis, See Reference 28.

Syntheses of Complexes for Comparative Studies

(L1)NiCl₂. NiCl₂(DME) (22.0 mg, 0.100 mmol, 1.0 equiv.) was suspended in DCM (1 mL). Ligand **L1** (36.7 mg, 0.100 mmol, 1.0 equiv.) was added dropwise to the suspension using additional DCM (3 mL). The reaction mixture was stirred for 1 h, during which time it became a yellow and homogeneous solution. The reaction mixture was filtered *via* syringe filter and concentrated to an orange solid. The solid was washed with pentane to yield the desired product as an orange, analytically pure solid (46.6 mg, 0.094 mmol, 94% yield). X-ray quality crystals of **(L1)NiCl₂** were grown from a saturated toluene solution at -35 °C. *Note*: This compound is air-stable. ¹H NMR (500 MHz, CD₂Cl₂): δ 7.89 – 7.74 (m, 4H, C₆H₅), 7.60 – 7.51 (m, 2H, C₆H₅), 7.49 – 7.42 (m, 4H, C₆H₅), 7.09 – 7.05 (m, 1H, pyrrole), 6.79 – 6.75 (m, 1H, pyrrole), 6.48 – 6.43 (m, 1H, pyrrole), 2.90 – 2.78 (m, 2H, CH(CH₃)₂), 1.52 (dd, *J* = 18.4, 7.1 Hz, 6H, CH₃), 1.37 (dd, *J* = 16.7, 7.1 Hz, 6H, CH₃). ¹³C NMR (126 MHz, CD₂Cl₂): δ 134.3 (d, *J* = 10.6 Hz), 132.1 (d, *J* = 2.9 Hz), 130.3, 129.8, 129.1 (d, *J* = 11.9 Hz), 126.1 (dd, *J* = 9.3, 4.1 Hz), 122.0 (dd, *J* = 6.7, 1.9 Hz), 118.6 (dd, *J* = 9.3, 3.8 Hz), 30.0 (d, *J* = 26.9 Hz), 19.1 (d, *J* = 2.4 Hz), 18.1 (d, *J* = 2.4 Hz). ³¹P NMR (202 MHz, CD₂Cl₂): δ 128.0 (d, *J* = 79.9 Hz), 18.8 (d, *J* = 79.7 Hz); **IR** (ATR, cm⁻¹): 2970, 2925, 1438, 1225, 1172, 1103, 747, 689, 653, 588, 535; **EA**: Anal. Calcd. for C₂₂H₂₇Cl₂NNiP₂: C, 53.17; H, 5.48; N, 2.82. Found: C, 53.04; H, 5.54; N, 2.59. **UV-vis** (CHCl₃): λ_{max} = 456 nm, ε₄₅₆ = 1.50 × 10³ M⁻¹cm⁻¹.

(L1)Ni(CO)₂. (Ph₃P)₂Ni(CO)₂ (38.4 mg, 0.060 mmol, 1.0 equiv.) was dissolved in THF (3 mL). Ligand **L1** (26.5 mg, 0.072 mmol, 1.2 equiv.) was added using additional THF (6 mL). The reaction mixture was stirred at 23 °C for 24 h, during which time it became a yellow and homogeneous solution. The reaction mixture was concentrated in the glovebox and was recrystallized from pentane at -35 °C overnight. The first crystallization yielded crystals of (Ph₃P)₂Ni(CO)₂ starting material. The reaction mixture was then pipetted into a second scintillation vial and placed in a freezer at -35 °C overnight. This second crystallization yielded the final product as colorless, spectroscopically pure crystals (11.0 mg, 0.023 mmol, 38% yield). *Note*: This compound is air-sensitive. ¹H NMR (500 MHz, CD₂Cl₂): δ 7.56 – 7.45 (m, 4H, C₆H₅), 7.38 – 7.32 (m, 6H, C₆H₅), 7.10 – 7.04 (m, 1H, pyrrole), 6.66 – 6.59 (m, 1H, pyrrole), 6.42 – 6.34 (m, 1H, pyrrole), 2.46 (dhept, *J* = 8.5, 6.9 Hz, 2H, CH(CH₃)₂), 1.14 (dd, *J* = 18.5, 6.9 Hz, 6H, CH₃), 0.80 (dd, *J* = 14.7, 6.9 Hz, 6H, CH₃). ¹³C NMR (126 MHz, CD₂Cl₂): δ 201.7 (dd, *J* = 7.2, 2.3 Hz), 138.0 (dd, *J* = 36.2, 5.0 Hz), 137.2 (dd, *J* = 61.7, 31.2 Hz), 132.5 (d, *J* = 14.8 Hz), 129.6 (d, *J* = 1.8 Hz), 128.8 (d, *J* = 9.7 Hz), 124.8 (dd, *J* = 7.4, 5.0 Hz), 118.1 (d, *J* = 4.9 Hz), 116.9 (d, *J* = 7.0 Hz), 30.3 (dd, *J* = 13.4, 3.9 Hz), 18.6 (d, *J* = 13.7 Hz), 17.9 (d, *J* = 2.8 Hz). ³¹P NMR (202 MHz, CD₂Cl₂): δ 127.12 (d, *J* = 6.1 Hz), 17.65 (d, *J* = 6.1 Hz). **IR** (ATR, cm⁻¹): 3062, 1996 (C=O), 1934 (C=O), 1477, 1434, 742, 695; **EA**: Anal. Calcd. for C₂₄H₂₇NNiO₂P₂: C, 59.79; H, 5.64; N, 2.91. Found: C, 58.23; H, 5.55; N, 2.77. Analytically pure material was not acquired despite multiple attempts.

(L11)NiCl₂. NiCl₂(DME) (22.0 mg, 0.100 mmol, 1.0 equiv.) was suspended in DCM (1 mL). Ligand **L11** (37.8 mg, 0.100 mmol, 1.0 equiv.) was transferred to the suspension using additional DCM (3 mL). The reaction mixture was stirred at 23 °C until homogenous (approx. 5 h), during which time the solution became orange. The reaction mixture was filtered *via* syringe filter and concentrated to an orange solid, which was then washed with pentane (approx. 3 mL). The desired product was isolated as orange analytically pure crystals (44.4 mg, 0.087 mmol, 87% yield) by diffusion of pentane to a DCE solution of **(L11)NiCl₂**. X-ray quality crystals were grown in the

same manner. *Note:* This compound is air-stable. **¹H NMR** (500 MHz, CD₂Cl₂): δ 7.84 – 7.77 (m, 4H), 7.75 – 7.70 (m, 1H), 7.68 – 7.62 (m, 1H), 7.62 – 7.51 (m, 3H), 7.49 – 7.39 (m, 5H), 2.90 – 2.76 (m, 2H), 1.51 (dd, *J* = 17.5, 7.0 Hz, 1H), 1.34 (dd, *J* = 16.0, 7.1 Hz, 1H). **¹³C NMR** (126 MHz, CD₂Cl₂): δ 143.9 (dd, *J* = 52.7, 31.7 Hz), 138.7 (dd, *J* = 40.2, 37.5 Hz), 134.4 (d, *J* = 10.1 Hz), 133.8 (dd, *J* = 13.8, 1.8 Hz), 133.4 (dd, *J* = 6.3, 2.1 Hz), 132.9 (dd, *J* = 5.3, 2.2 Hz), 132.28 – 131.81 (m), 130.32 (d, *J* = 55.5 Hz), 129.2 (d, *J* = 11.2 Hz), 28.0 (d, *J* = 27.0 Hz), 19.8 (d, *J* = 2.2 Hz), 18.8 (d, *J* = 2.1 Hz); **³¹P NMR** (202 MHz, CD₂Cl₂): δ 84.4 (d, *J* = 71.0 Hz), 55.2 (d, *J* = 70.3 Hz); **IR** (ATR, cm⁻¹): 2967, 2923, 2869, 1439, 1249, 1100, 747, 700, 547; **EA:** Anal. Calcd. for C₂₄H₂₈Cl₂NiP₂: C, 56.74; H, 5.56, N: 0.00. Found: C, 56.35; H, 5.03; N, 0.00. **UV-vis** (CHCl₃): λ_{max} = 454 nm, ε₄₅₆ = 1.52 × 10³ M⁻¹cm⁻¹.

(L11)Ni(CO)₂. (Ph₃P)₂Ni(CO)₂ (38.4 mg, 0.060 mmol, 1.0 equiv.) was dissolved in THF (3 mL) in a 20-mL scintillation vial. Ligand **L1** (25.0 mg, 0.066 mmol, 1.1 equiv.) was added to the nickel solution using additional THF (6 mL). The reaction mixture was sealed, removed from the glovebox, and heated at 50 °C for 22 h, during which time it became a light yellow, homogeneous solution. (*Note:* Elevated temperatures were required to ensure complete consumption of nickel starting material) The reaction mixture was opened to air and concentrated under reduced pressure. The product was isolated as a spectroscopically pure, colorless solid (18.8 mg, 0.064 mmol, 64% yield) following two recrystallizations from pentane at -25 °C. *Note:* This compound is air-stable. **¹H NMR** (500 MHz, CD₂Cl₂): δ 7.74 – 7.69 (m, 1H, phenylene), 7.51 – 7.46 (m, 1H, phenylene), 7.44 – 7.30 (m, 12H), 2.41 (dhept, *J* = 9.3, 6.9 Hz, 2H), 1.14 (dd, *J* = 16.9, 6.9 Hz, 6H), 0.76 (dd, *J* = 14.5, 6.9 Hz, 6H). **¹³C NMR** (126 MHz, CD₂Cl₂): δ 202.6 (t, *J* = 4.1 Hz), 146.7 (t, *J* = 39.0 Hz), 145.4 (dd, *J* = 44.5, 30.0 Hz), 138.4 (dd, *J* = 27.9, 6.2 Hz), 134.2 (d, *J* = 11.6 Hz), 132.6 (d, *J* = 14.3 Hz), 131.1 (d, *J* = 13.5 Hz), 130.3 (t, *J* = 5.2 Hz), 129.4 (d, *J* = 1.7 Hz), 128.8 (d, *J* = 9.1 Hz), 27.7 (dd, *J* = 15.1, 5.5 Hz), 19.9 (d, *J* = 10.8 Hz), 19.0 (d, *J* = 3.7 Hz) (*Note:* One aromatic signal was not observed); **³¹P NMR** (202 MHz, CD₂Cl₂): δ 76.1 (d, *J* = 24.8 Hz), 47.7 (d, *J* = 25.1 Hz); **IR** (ATR, cm⁻¹): 2693, 1986 (C=O), 1923 (C=O), 1438, 744, 629; **EA:** Anal. Calcd. for C₂₆H₂₈NiO₂P₂: C, 63.32; H, 5.72; N, 0.00. Found: C, 62.54; H, 6.01; N, 0.00. Combustion analysis was low in carbon despite multiple attempts.

Buried Volume Details for (L1)NiCl₂ and (L11)NiCl₂

Buried volume (% *V*_{bur}) calculations were performed for both (L1)NiCl₂ and (L11)NiCl₂ using the SambVca 2.0 web application⁹ and the solid state structures of each compound based on the following parameters:

Atomic radii: 1.17, *Sphere radius:* 3.5, *Mesh:* 0.10, *H Atoms:* included

Nickel and chloride atoms were omitted for each calculation.

Synthesis of L1 Precatalyst, C1

(L1)Ni(*o*-tolyl)Cl. A 20-mL scintillation vial was charged with **L1** (38.6 mg, 0.105 mmol, 1.05 equiv.), (TMEDA)Ni(*o*-tolyl)Cl (30.1 mg, 0.100 mmol, 1.0 equiv), and THF (4 mL). The vial was sealed, removed from the glovebox, and heated at 50 °C for 3 h. The orange, homogeneous reaction mixture was opened to air and concentrated by rotary evaporation. The resulting orange foam was

dissolved in DCM, filtered, and concentrated to approximately ~0.5 mL. To the solution was added pentane (~15 mL), which immediately resulted in a turbid solution. The solution was stored at -35 °C to induce crystallization. The product was isolated as orange crystals (42.4 mg, 0.077 mmol, 77% yield). X-ray quality crystals were grown from a dilute DCM/pentane solution (~1:15) at -35 °C. *Note:* This complex is air-stable. ¹H NMR (500 MHz, CD₂Cl₂): δ 8.01 – 7.94 (m, 2H), 7.51 – 7.37 (m, 4H), 7.16 – 7.06 (m, 4H), 6.70 – 6.62 (m, 4H), 6.57 – 6.48 (m, 2H), 6.29 – 6.26 (m, 1 H), 2.86 – 2.74 (m, 2H), 2.08 (s, 3H), 1.63 – 1.44 (m, 3H), 1.32 (ddd, *J* = 14.5, 7.0, 2.0 Hz, 6H). ¹³C NMR (126 MHz, CD₂Cl₂): δ 157.2 (dd, *J* = 91.8, 39.5 Hz), 145.2, 138.2 – 137.5 (m), 137.3 – 137.1 (m), 133.7 (dd, *J* = 95.5, 10.9 Hz), 132.5 (d, *J* = 60.9 Hz), 131.4 (d, *J* = 2.8 Hz), 130.8 (d, *J* = 2.8 Hz), 129.6 – 129.1 (m) 128.7 (dd, *J* = 134.3, 11.1 Hz), 125.7 (dd, *J* = 7.9, 5.3 Hz), 123.3 (d, *J* = 3.2 Hz), 120.4 (d, *J* = 6.2 Hz), 117.4 (dd, *J* = 9.4, 3.1 Hz), 27.7 (dd, *J* = 58.1, 15.6 Hz), 24.6 (d, *J* = 2.0 Hz), 18.6 (dd, *J* = 36.1, 5.7 Hz), 18.1 (d, *J* = 22.5 Hz). ³¹P NMR (202 MHz, CD₂Cl₂): δ 111.7 (d, *J* = 34.4 Hz), 21.9 (d, *J* = 33.7 Hz). IR (ATR, cm⁻¹): 3056, 2960, 1571, 1436, 1217, 1177, 1100, 1057, 1026, 959, 882, 740, 694, 574. EA: Anal. Calcd. for C₂₉H₃₄ClNNiP₂: C, 63.03; H, 6.20; N, 2.53. Found: C, 62.92; H, 6.31; N, 2.62.

Catalytic Studies

A 20-mL scintillation vial was charged with 4-chlorobenzonitrile (34.4 mg, 0.250 mmol, 1.0 equiv.), furfurylamine (25 μL, 0.0282 mmol), (**L#**)Ni(*o*-tolyl)Cl (6.5 mg, 0.012 mmol, 5 mol%), NaO*t*-Bu (48.1 mg, 0.501 mmol, 2.0 equiv.), and toluene (2.5 mL). The vial was sealed, removed from the glovebox, and heated at the reported temperature for 16 h in a temperature-controlled aluminum block. The reaction mixture was filtered through cotton and then a syringe filter, each of which was washed with DCM. A chloroform solution of ferrocene (1.0 mL, 0.0250 M) was added to the filtered reaction mixture. An aliquot of the new solution was concentrated by rotary evaporation and analyzed by ¹H NMR spectroscopy to determine the yield.

Acknowledgements

This work was supported by the Arnold and Mabel Beckman Foundation, the National Science Foundation, the Petroleum Research Fund, and the University of Richmond School of Arts and Sciences. Other contributors include Hilary Fokwa, Sophie Weinberg, and Isaiah Duplessis who aided in the synthesis of the ligand library, and Sadie Taylor who obtained X-ray quality crystals of **C3**. I would also like to thank Dr. Michael Norris (University of Richmond) for assistance with electrochemical studies, Dr. Julie Pollock (University of Richmond) for assistance with UV-Vis, and Dr. Nathan Schley (Vanderbilt University) for performing the X-ray crystallography analysis. Finally, I would like to thank Dr. Miles Johnson whose encouragement and support guided me throughout this project and helped make this work possible.

References

- (1) Johansson Seechurn, C. C. C.; Kitching, M. O.; Colacot, T. J.; Snieckus, V. Palladium-Catalyzed Cross-Coupling: A Historical Contextual Perspective to the 2010 Nobel Prize. *Angew. Chem. Int. Ed.* **2012**, *51*, 5062–5085.
- (2) Guram, A. S.; Rennels, R. A.; Buchwald, S. L. A Simple Catalytic Method for the Conversion of Aryl Bromides to Arylamines. *Angew. Chem. Int. Ed. Engl.* **1995**, *34*, 1348–1350.

- (3) Louie, J.; Hartwig, J. F. Palladium-catalyzed Synthesis of Arylamines from Aryl Halides. Mechanistic Studies Lead to Coupling in the Absence of Tin Reagents. *Tetrahedron Lett.* **1995**, *36*, 3609–3612.
- (4) Ruiz-Castillo, P.; Buchwald, S. L. Applications of Palladium-Catalyzed C–N Cross-Coupling Reactions. *Chem. Rev.* **2016**, *116*, 12564–12649.
- (5) Brown, D. G.; Boström, J. Analysis of Past and Present Synthetic Methodologies on Medicinal Chemistry: Where Have All the New Reactions Gone? *J. Med. Chem.* **2016**, *59*, 4443–4458.
- (6) Wedepohl, K. H. The Composition of the Continental Crust. *Geochim. Cosmochim. Acta.* **1995**, *59*, 1217–1232.
- (7) Hayler, J. D.; Leahy, D. K.; Simmons, E. M. A Pharmaceutical Industry Perspective on Sustainable Metal Catalysis. *Organometallics* **2018**, *38*, 36–46.
- (8) Diccianni, J. B.; Diao, T. Mechanisms of Nickel-Catalyzed Cross-Coupling Reactions. *Trends in Chem.* **2019**, *1*, 830–844.
- (9) Schwarzer, M. C.; Konno, R.; Takayuki, H.; Ohtsuki, A.; Nakamura, K.; Yasutome, A.; Takahashi, H.; Shimasaki, T.; Tobisu, M.; Chatani, N.; Mori, S. Combined Theoretical and Experimental Studies of Nickel-Catalyzed Cross-Coupling of Methoxyarenes with Arylboronic Esters via C–O Bond Cleavage. *J. Am. Chem. Soc.* **2017**, *139*, 10347–10358.
- (10) Somerville, R.J.; Hale, L. V. A.; Gómez-Bengoña E.; Burés, J.; Martin, R. Intermediacy of Ni–Ni Species in sp² C–O Bond Cleavage of Aryl Esters: Relevance in Catalytic C–Si Bond Formation. *J. Am. Chem. Soc.* **2018**, *140*, 8771–8780.
- (11) Park, N. H.; Teverovskiy, G.; Buchwald, S. L. Development of an Air-Stable Nickel Precatalyst for the Amination of Aryl Chlorides, Sulfamates, Mesylates, and Triflates. *Org. Lett.* **2014**, *16*, 220–223.
- (12) Ge, S. Z.; Green, R. A.; Hartwig, J. F. Controlling First-Row Catalysts: Amination of Aryl and Heteroaryl Chlorides and Bromides with Primary Aliphatic Amines Catalyzed by a BINAP-Ligated Single-Component Ni(0) Complex. *J. Am. Chem. Soc.* **2014**, *136*, 1617–1627.
- (13) Lavoie, C. M.; Stradiotto, M. Bisphosphines: A Prominent Ancillary Ligand Class for Application in Nickel-Catalyzed C–N Cross-Coupling. *ACS Catal.* **2018**, *8*, 7228–7250.
- (14) Liu, R.Y.; Dennis, J. M.; Buchwald, S. L. The Quest for the Ideal Base: Rational Design of a Nickel Precatalyst Enables Mild, Homogeneous C–N Cross-coupling. *J. Am. Chem. Soc.* **2020**, *142*, 4500–4507.
- (15) Lavoie, C. M.; MacQueen, P. M.; Rotta-Loria, N. L.; Sawatzky, R. S.; Borzenko, A.; Chisholm, A. J.; Hargreaves, B. K. V.; McDonald, R.; Ferguson, M. J.; Stradiotto, M. Challenging Nickel-Catalysed Amine Arylations Enabled by Tailored Ancillary Ligand Design. *Nat. Commun.* **2016**, *7*, 1–11.
- (16) Clark, J. S.; McGuire, R. T.; Lavoie, C. M.; Ferguson, M. J.; Stradiotto, M. Examining the Impact of Heteroaryl Variants of PAd-DalPhos on Nickel-Catalyzed C(sp²)-N Cross-Couplings. *Organometallics* **2019**, *38*, 167–175.
- (17) Clark, J. S.; Ferguson, M. J.; McDonald, R.; Stradiotto, M. PAd₂-DalPhos Enables the Nickel-Catalyzed C–N Cross-Coupling of Primary Heteroarylamines and (Hetero) aryl Chlorides. *Angew. Chem.* **2019**, *131*, 6457–6461.
- (18) McGuire, R. T.; Paffile, J. F.; Zhou, Y.; Stradiotto, M. Nickel-catalyzed C–N Cross-coupling of Ammonia, (Hetero) Anilines, and Indoles with Activated (Hetero) Aryl Chlorides Enabled by Ligand Design. *ACS Catal.* **2019**, *9*, 9292–9297.

- (19) Dunn, P. L.; Reath, A. H.; Clouston, L. J.; Young, V. G.; Tonks, I. A. Homo- and Heteroleptic Group 4 2-(Diphenylphosphino)Pyrrolide Complexes: Synthesis, Coordination Chemistry and Solution State Dynamics. *Polyhedron* **2014**, *84*, 111–119.
- (20) Bedford, R. B.; Brenner, P. B.; Carter, E.; Clifton, J.; Cogswell, P. M.; Gower, N. J.; Haddow, M. F.; Harvey, J. N.; Kehl, J. A.; Murphy, D. M.; Neeve, E. C.; Neidig, M. L.; Nunn, J.; Snyder, B. E. R.; Taylor, J. Iron Phosphine Catalyzed Cross-Coupling of Tetraorganoborates and Related Group 13 Nucleophiles with Alkyl Halides. *Organometallics* **2014**, *33*, 5767–5780.
- (21) Falivene, L.; Cao, Z.; Petta, A.; Serra, L.; Poater, A.; Oliva, R.; Scarano, V.; Cavallo, L. Towards the Online Computer-aided Design of Catalytic Pockets. *Nat. Chem.* **2019**, *11*, 872–879.
- (22) Shields, J. D.; Gray, E. E.; Doyle, A. G. A Modular, Air-Stable Nickel Precatalyst. *Org. Lett.* **2015**, *17*, 2166–2169.
- (23) Clark, J. S. K.; Voth, C. N.; Ferguson, M. J.; Stradiotto, M. Evaluating 1,1'-Bis(Phosphino)Ferrocene Ancillary Ligand Variants in the Nickel-Catalyzed C–N Cross-Coupling of (Hetero)Aryl Chlorides. *Organometallics* **2017**, *36*, 679–686.
- (24) Gatien, A. V.; Lavoie, C. M.; Bennett, R. N.; Ferguson, M. J.; McDonald, R.; Johnson, E. R.; Speed, A. W. H.; Stradiotto, M. Application of Diazaphospholidine/Diazaphospholene-Based Bisphosphines in Room-Temperature Nickel-Catalyzed C(Sp²)–N Cross-Couplings of Primary Alkylamines with (Hetero)Aryl Chlorides and Bromides. *ACS Catal.* **2018**, *8*, 5328–5339.
- (25) McGuire, R. T.; Clark, J. S. K.; Gatien, A. V.; Shen, M. Y.; Ferguson, M. J.; Stradiotto, M. Bulky 1,1'-Ferrocenyl Ligands Featuring Diazaphospholene or Dioxaphosphepine Donor Fragments: Catalytic Screening in Nickel-Catalyzed C–N Cross-Coupling. *Eur. J. Inorg. Chem.* **2019**, *38*, 4112–4116.
- (26) Clark, J. S. K.; Ferguson, M. J.; McDonald, R.; Stradiotto, M. PAd₂-DalPhos Enables the Nickel-Catalyzed C–N Cross-Coupling of Primary Heteroarylamines and (Hetero)Aryl Chlorides. *Angew. Chem. Int. Ed.* **2019**, *58*, 6391–6395.
- (27) Clark, J. S. K.; McGuire, R. T.; Lavoie, C. M.; Ferguson, M. J.; Stradiotto, M. Examining the Impact of Heteroaryl Variants of PAd-DalPhos on Nickel-Catalyzed C(Sp²)-N Cross-Couplings. *Organometallics* **2019**, *38*, 167–175.
- (28) Fokwa, H. D.; Vidlak, J. F.; Weinberg, S. C.; Duplessis, I. D.; Schley, N. D.; Johnson, M. W. Study and Modular Synthesis of Unsymmetrical Bis(phosphino)pyrrole Ligands. *Dalton Trans.* **2020**, *49*, 9957–9960.
- (29) Tolman, C. A. Steric Effects of Phosphorus Ligands in Organometallic Chemistry and Homogenous Catalysis. *Chem. Rev.* **1977**, *77*, 313–348.
- (30) Stephens, P. J.; Devlin, F. J.; Chabalowski, C. F.; Frisch, M. J. Ab Initio Calculation of Vibrational Absorption and Circular Dichroism Spectra Using Density Functional Force Fields. *J. Phys. Chem.* **1994**, *98*, 11623–11627.
- (31) Becke, A. D. Density-functional Thermochemistry. III. The Role of Exact Exchange. *J. Chem. Phys.* **1993**, *98*, 5648–5652.
- (32) Dunning, T. H. Gaussian Basis Sets for Use in Correlated Molecular Calculations. I. The Atoms Boron through Neon and Hydrogen. *J. Chem. Phys.* **1989**, *90*, 1007–1023.
- (33) Peterson, K. A.; Woon, D. E.; Dunning, T. H. Benchmark Calculations with Correlated Molecular Wave Functions. IV. The Classical Barrier Height of the H+H₂→H₂+H Reaction. *J. Chem. Phys.* **1994**, *100*, 7410–7415.